

Modeling Spacer Dynamics during Ice-Shedding-Induced Vibrations

László E. Kollár and Masoud Farzaneh

NSERC/Hydro-Québec/UQAC Industrial Chair on Atmospheric Icing of Power Network Equipment (CIGELE) and Canada Research Chair on Atmospheric Icing Engineering of Power Networks (INGIVRE) at Université du Québec à Chicoutimi, Chicoutimi, Québec, Canada, G7H 2B1
<http://www.cigele.ca>, Laszlo_Kollar@uqac.ca, Masoud_Farzaneh@uqac.ca

Abstract—Ice and snow shedding from conductors and cables may result in high-amplitude vibrations and dynamic forces damaging to the power lines. The application of spacers in conductor bundles reduces the severity of vibration; however, it increases cable tension and stress in the neighborhood of the spacer clamps. Moreover, the spacers themselves are exposed to excessive dynamic forces. A four-degree-of-freedom model has been developed to simulate ice-shedding-induced vibration of the spacer including its attachment points unto the cable. Although this model considers the vertical plane of the spacer only, it implies the dynamic effects of the whole set of cables in the span. The model is compared to a formerly developed model of vibrating bundled conductors in terms of the maximum vertical displacement of the cable at the spacer clamp during the vibration. The proposed model can be used to calculate the rotation of the spacer and the forces acting on it during the vibration, and thus, to predict when the vibration results in damaging dynamic forces.

I. INTRODUCTION

SPACERS and spacer dampers are often used in transmission lines in order to maintain the distance between individual conductors in a bundle. Spacers were used for electrical reasons originally, but they also help to attenuate vibrations, since they create shorter subspans as compared to the length of the whole span; moreover, spacer dampers possess elastic and damping properties. Vibrations may arise due to several reasons such as wind load, ice shedding or conductor breakage. The maximum forces during these vibrations act at the suspension as well as near the spacer clamp. Phenomena leading to asymmetric dynamic loads like ice shedding from one subconductor or conductor breakage cause the rotation of the bundle, and thereby increase dynamic forces. Thus, the determination of bundle rotation is also of interest when studying the dynamics of bundled conductors. The present paper deals with the dynamic behavior of twin bundles in the neighborhood of the spacer following ice shedding from one subconductor.

Vibration of transmission line cables, including ice-shedding-induced vibration and its modeling have been the subject of many publications. A series of load-dropping tests were carried out in [1] to simulate ice shedding and obtain the maximum jump height arising during the resulting vibration. McClure and collaborators [2], [3] applied the commercial finite element analysis software, ADINA [4], for modeling ice shedding from a single span of transmission lines. Previous

studies of the present authors also used the finite element method to model ice shedding from a single span considering the mechanical properties of ice [5], and to simulate the vibrations following ice shedding from bundled conductors [6]. The latter model considered vibrations in the vertical plane; it did not predict, however, the rotation of the bundle. Reference [7] developed a mathematical model to simulate vortex-induced vibrations in bundled conductors with spacer dampers, and computed forces at the spacer connection and maximum bending strains in a conductor. The present paper introduces a four degree-of-freedom (DOF) model of a twin bundle in the plane of the spacer and simulates ice-shedding-induced vibrations. This model does not provide information about the cable vibration along its entire length, but it includes the dynamic effects of the whole set of cables, and thus, it is applicable to determine the rotation of the spacer and the forces acting on it.

II. SPACERS

Typical spacers consist of a rigid central frame and arms which are attached to the central frame by flexible joints. The free end of each arm is clamped to one subconductor. The elastic properties of such spacers lie in the flexibility of the joints. Arms are allowed to rotate a few degrees around the joint with increasing resistance until the rotating part will be blocked and further deformation will only be possible by the elongation of spacer material. A recent survey on spacers including types, materials, design characteristics, test methods and field experience is presented in [8]. Fig. 1 shows a spacer which is used in twin bundles.



Fig. 1. Spacer in a twin bundle of a transmission line

III. CONSTRUCTION OF THE 4-DOF MODEL

The 4-DOF model of a spacer in a twin bundle is sketched in Fig. 2. The conductors are hanging in the y - z plane, whereas the spacer connects them at mid-span perpendicularly to that plane. The model simulates vibration in the x - z plane only. Symbols m_1 and m_2 stand for the mass of the ice-loaded cables. The elasticity of the spacer and cables (or cable-ice compositions) in the vertical direction is modeled by nonlinear springs. The vector $\mathbf{c}_s = (c_{s0} \ c_{s1} \ c_{s2} \ c_{s3})^T$ includes the spring constants describing the elasticity of the spacer. The elasticity of cables in the vertical direction is represented by springs with constants included in the vectors $\mathbf{c}_1 = (c_{10} \ c_{11} \ c_{12} \ c_{13})^T$ and $\mathbf{c}_2 = (c_{20} \ c_{21} \ c_{22} \ c_{23})^T$. The elasticity of cables in the transverse direction may be modeled satisfactorily by a linear spring; thus, single constants, c_{x1} and c_{x2} , describe the elasticity of two cables in the transverse direction. The damping vectors $\mathbf{d}_1 = (d_{11} \ d_{12})^T$ and $\mathbf{d}_2 = (d_{21} \ d_{22})^T$ consist of constants accounting for structural damping, d_{11} and d_{21} , and for aerodynamic damping, d_{12} and d_{22} , of cables in the vertical direction; whereas the vectors $\mathbf{d}_{x1} = (d_{x11} \ d_{x12})^T$ and $\mathbf{d}_{x2} = (d_{x21} \ d_{x22})^T$ include constants accounting for the damping of cables in the transverse direction. The structural damping of the spacer is also considered, the corresponding damping constant being d_s . The general coordinates of the system are the transverse displacements of the masses, x_1 and x_2 ; as well as the vertical distance from the suspension point, z_1 and z_2 , where $z_1 = z_{10} + \Delta z_1$ and $z_2 = z_{20} + \Delta z_2$ with z_{10} and z_{20} describing the sag of the ice-loaded cables in equilibrium, and Δz_1 and Δz_2 denoting the vertical displacements of m_1 and m_2 . Before constructing the equations of motion, the mass, spring and damping constants have to be determined.

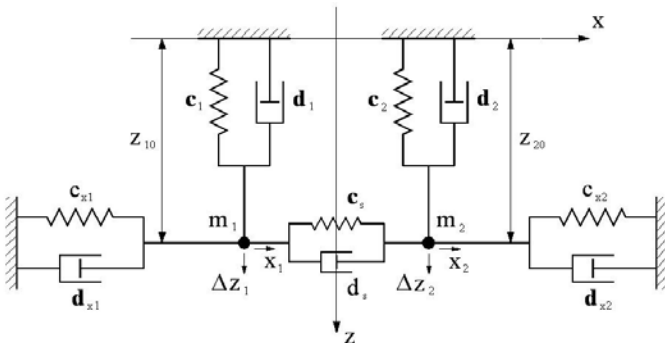


Fig. 2. The 4-DOF model of spacer in a twin bundle

A. Mass of Iced Cable

The mass of the iced cable, m_{ci} , is calculated from the following formula:

$$m_{ci} = \left[\mu_i + \rho_{ice} \frac{(D_i + 2b_i)^2 - D_i^2}{4} \pi \right] L, \quad i=1,2 \quad (1)$$

where μ is mass per unit length, ρ_{ice} is density of ice, D is diameter of bare cable, b is thickness of ice accumulation which is assumed to be circular, L is length of the span, and the index i refers to subconductors in the bundle. If cable i is bare, then $b_i = 0$, and (1) is simplified as follows: $m_{ci} = \mu_i L$. The mass of the spacer is approximated by the following expression:

$$m_s = A_s l_s \rho_s \quad (2)$$

where A_s , l_s , ρ_s are the cross-sectional area, the length and density of spacer, respectively. The spacer mass is added to the mass of the iced cable as follows:

$$m_i = m_{ci} + \frac{m_s}{2}, \quad i=1,2 \quad (3)$$

This simplification does not cause any noticeable difference in the results, because the mass of the spacer is two to three orders of magnitude less than that of the iced cable.

B. Spring Constants of Cable-Ice Composition

The spring constants of the cable-ice composition are determined by applying the statics of suspended cables [9]. The calculation is carried out in three steps. First, the horizontal component of initial tension in the bare cable is determined; then, the displacement due to uniformly distributed ice load is computed at the midpoint of the span where the spacer is assumed; and finally, the displacement – load relationship is derived given the application of a point load at mid-span of the iced cable.

The initial tension in the bare cable, H , is obtained by solving the following equation:

$$f = \frac{H}{\mu g} \left[\cosh\left(\frac{\mu g L}{2H}\right) - 1 \right] \quad (4)$$

with f denoting the sag of the span, which is prescribed, and g the gravitational constant. Note that the calculation presented in this section is the same for the two cables, thus index i is omitted for simplification.

The additional displacement at the midpoint of the span, w_d , due to a uniformly distributed load, p , is provided by the expression:

$$w_d \left(\frac{L}{2} \right) = \frac{pL^2}{8(H + h_d)} \left(1 - \frac{\mu g h_d}{pH} \right) \quad (5)$$

where h_d is the additional tension owing to the distributed load, and obtained from the third order equation:

$$h_d^3 + \left(2 + \frac{\lambda^2}{24} \right) H h_d^2 + \left(1 + \frac{\lambda^2}{12} \right) H^2 h_d - \frac{\lambda^2}{12} \frac{pH^3}{\mu g} \left(1 + \frac{p}{2\mu g} \right) = 0 \quad (6)$$

with $\lambda^2 = (\mu g L / H)^2 L / (H L_c / EA)$. The sag and the additional

displacement determine the initial configuration of the system, in which $z_0 = f + w_d$.

During cable vibration a point load is applied on the cables at mid-span from the spacer. The relationship between the resulting additional vertical displacement, w_p , and the vertical component of force, P_z , may be obtained from the vertical equilibrium of the cable and the cable equation, and is described by the formula:

$$w_p = \frac{P_z L}{4(\tilde{H} + h_{pz})} \left(1 - \frac{\tilde{\mu} g L h_{pz}}{2P\tilde{H}} \right) \quad (7)$$

where the increment in the cable tension, h_{pz} , due to the point load is obtained from a third order equation:

$$h_{pz}^3 + \left(2 + \frac{\tilde{\lambda}^2}{24} \right) \tilde{H} h_{pz}^2 + \left(1 + \frac{\tilde{\lambda}^2}{12} \right) \tilde{H}^2 h_{pz} - \tilde{\lambda}^2 \frac{P_z \tilde{H}^3}{8\tilde{\mu} g L} \left(1 + \frac{P_z}{\tilde{\mu} g L} \right) = 0 \quad (8)$$

with $\tilde{H} = H + h_d$, $\tilde{\mu} = \mu + \rho_{ice} \pi ((D + 2b)^2 - D^2)/4$, and $\tilde{\lambda}^2 = (\mu g L / H)^2 L / (H L_e / EA)$. In the range of $-3 \leq w_p \leq 3$, the dependence $P_z(w_p)$ may closely be approximated by a third order polynomial. Since neither the cable jump nor its drop exceeds 3 m in the cases considered in this project, a third-order-polynomial fit is applied to express the point load – additional vertical displacement relationship, $P_z(w_p)$. Then, the spring force – vertical displacement relationship, $F_{cz}(z)$, is obtained after applying the following transformation: $z = z_0 + w_p$ and $F_{cz} = -P_z - mg$. Thus, the spring constants in the vectors \mathbf{c}_1 and \mathbf{c}_2 are defined as follows:

$$F_{czi} = c_{i0} + c_{i1} z_i + c_{i2} z_i^2 + c_{i3} z_i^3, \quad i=1,2 \quad (9)$$

The spring constants describing the elasticity of cable-ice compositions in the transverse direction are obtained from the relationship between the transverse component of the point load, P_x , and the displacement, u_p , caused by this load. If the vertical displacement due to the transverse load is neglected, then this relationship may be derived in a similar way as that between the vertical load, P_z , and the resulting vertical displacement, w_p , to obtain

$$u_p = \frac{P_x L}{4(\tilde{H} + h_{px})} \quad (10)$$

where the additional cable tension, h_{px} , due to the load, P_x , is calculated from the following equation:

$$h_{px}^3 + 2\tilde{H} h_{px}^2 + \tilde{H}^2 h_{px} - \frac{\tilde{H}^3 \tilde{\lambda}^2 P_x^2}{8(\tilde{\mu} g L)^2} = 0 \quad (11)$$

The transverse motion of cables does not exceed the range of

the distance between subconductors, i.e. l_s , where a linear approximation is satisfactory. Then, the spring force – transverse displacement relationship may simply be written as:

$$F_{cxi} = -c_{xi} x_i, \quad i=1,2 \quad (12)$$

C. Spring Constants of Spacer

Owing to the performance of spacers, such as the one shown in Fig. 1, the elastic properties of spacer should be modeled by a nonlinear spring rather than a linear one. More precisely, spring characteristics consist of two parts: (i) a cubic function until a critical deformation at which the rotation of the arms is blocked, and (ii) a linear function in the region where further deformation is possible only by elongation of the spacer material (see Fig. 3). If it is assumed that the value of the cubic function is zero for zero deformation and so is its tangent, and furthermore that the cubic function has inflexion at zero, then the constants c_{s0} , c_{s1} and c_{s2} are all zero in the cubic part. The only nonzero constant is obtained from the condition that the tangents of the two parts at the connection should be identical, and equal to $E_s A_s / l_s$. Thus, $c_{s3} = E_s A_s / (3l_s \Delta l_{cr}^2)$, with E_s denoting Young's modulus of spacer in the linear part. The symbol Δl refers to the elongation of the spacer, and it is related to the general coordinates as follows:

$$\Delta l = l_1 - l_s \quad (13)$$

where $l_1 = \sqrt{(l_s + x_2 - x_1)^2 + (\Delta z_1 - \Delta z_2)^2}$. If the same ice load is assumed on the two cables initially, i.e. $z_{10} = z_{20}$, then $l_1 = \sqrt{(l_s + x_2 - x_1)^2 + (z_1 - z_2)^2}$. If the angle of spacer rotation until the arms are blocked is φ_{cr} , then the corresponding elongation is obtained as follows:

$$\Delta l_{cr} = \frac{l_s}{\cos \varphi_{cr}} - l_s \quad (14)$$

The constants, c_{s2} and c_{s3} , are zero in the linear part, the constant c_{s1} is equal to $E_s A_s / l_s$, and the constant c_{s0} is obtained from the condition that the cubic and linear functions take the same value at the connection; thus $c_{s0} = -2E_s A_s \Delta l_{cr} / (3l_s)$. Therefore, the force – displacement

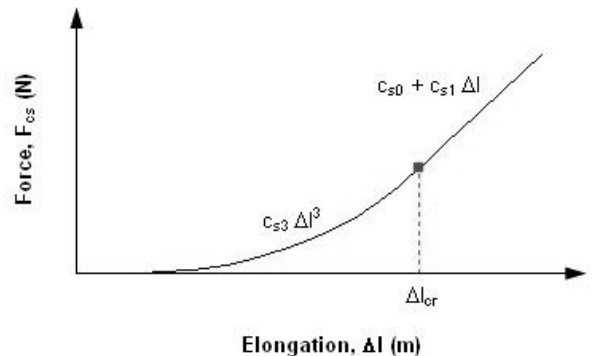


Fig. 3. Spring characteristics of spacer

relationship, $F_{cs}(\Delta l)$, is defined as follows:

$$F_{cs} = \begin{cases} c_{s3}\Delta l^3 & \text{if } \Delta l < \Delta l_{cr} \\ c_{s0} + c_{s1}\Delta l & \text{if } \Delta l \geq \Delta l_{cr} \end{cases} \quad (15)$$

D. Structural Damping and Aerodynamic Damping

The damping forces which result from the structural damping of the cables are proportional to the velocity of masses m_1 and m_2 . The damping constants d_{11} and d_{21} are calculated from the formula:

$$d_{i1} = 2\xi_i \sqrt{A_i E_i \mu_i + \left(\frac{(D_i + 2b_i)^2 - D_i^2}{4} \right)^2 E_{ice} \rho_{ice}}, \quad i=1,2 \quad (16)$$

where ξ is damping ratio, A and E are cross sectional area and Young's modulus of cable, respectively, and E_{ice} is Young's modulus of ice.

The damping force owing to aerodynamic damping is proportional to the square of velocity. The damping constants d_{12} and d_{22} are determined as follows:

$$d_{i2} = \frac{1}{2} C_{Di} \rho A_{pi}, \quad i=1,2 \quad (17)$$

where the symbols C_D and ρ stand for drag coefficient and air density, respectively, whereas $A_p = (D + 2b)L$ is the projected area of the iced cable. Then the total damping force may be written in the form:

$$F_{dzi} = -d_{i1}\dot{z}_i - d_{i2}\dot{z}_i^2, \quad i=1,2 \quad (18)$$

Damping constants in the transverse direction are determined in the same way, and so, the damping force in the transverse direction takes the form:

$$F_{dxi} = -d_{xi1}\dot{x}_i - d_{xi2}\dot{x}_i^2, \quad i=1,2 \quad (19)$$

The structural damping of spacer is calculated from a formula similar to (16), with the spacer assumed to be ice free:

$$d_s = 2\xi_s \sqrt{E_{s0} A_s^2 \rho_s} \quad (20)$$

where E_{s0} is approximated as the tangent of the line drawn between the origin and the connection point of the cubic and the linear part of the stress-strain curve. The damping force has the following form:

$$F_{ds} = d_s \dot{l} \quad (21)$$

E. Equations of Motion

The equations of motion of the system may be obtained by means of the Lagrangian equations of the second kind

$$\frac{d}{dt} \frac{\partial T}{\partial \dot{q}_k} - \frac{\partial T}{\partial q_k} = Q_k, \quad k=1, \dots, 4 \quad (22)$$

where $q_1 = x_1$, $q_2 = x_2$, $q_3 = z_1$ and $q_4 = z_2$ are the general coordinates,

$$T = \frac{1}{2} m_1 (\dot{x}_1^2 + \dot{z}_1^2) + \frac{1}{2} m_2 (\dot{x}_2^2 + \dot{z}_2^2) \quad (23)$$

is the kinetic energy, and Q_k is the general force including the spring forces, damping forces and gravity:

$$\begin{aligned} Q_1 &= F_{cx1} + F_{cs} \cos \varphi + F_{dx1} + F_{ds} \cos \varphi \\ Q_2 &= F_{cx2} - F_{cs} \sin \varphi + F_{dx2} - F_{ds} \sin \varphi \\ Q_3 &= F_{cz1} - F_{cs} \cos \varphi + F_{dz1} - F_{ds} \cos \varphi + m_1 g \\ Q_4 &= F_{cz2} + F_{cs} \sin \varphi + F_{dz2} + F_{ds} \sin \varphi + m_2 g \end{aligned} \quad (24a-d)$$

where φ is the angle of spacer rotation. If the same ice load is assumed on the two cables initially, then

$$\cos \varphi = \frac{l_s + x_2 - x_1}{l_1} \quad \text{and} \quad \sin \varphi = \frac{z_1 - z_2}{l_1} \quad (25a-b)$$

IV. SIMULATION OF ICE SHEDDING FROM ONE SUBCONDUCTOR IN A TWIN BUNDLE

Results of simulating ice shedding from either subconductor in a twin bundle are presented in this section. First, parameter values need to be specified; then the model has to be compared to a finite element model developed in a previous study [6] by means of vibration amplitudes; and, finally, the rotation of the bundle and the force acting on the spacer has to be determined for different values of ice thickness.

A. Parameter Values

The twin bundle considered in the model consists of two identical Bersfort conductors, thus, the cable parameters listed in Table 1 are the same for the two cables.

TABLE I
CABLE PARAMETERS

Cable parameter	Symbol and unit	Value
Diameter	D (mm)	35.6
Cross sectional area	A (mm ²)	747.1
Length	L (m)	200
Mass per unit length	μ (kg/m)	2.37
Young's modulus	E (GPa)	67.6

The damping ratio of cables is assumed to be 2% in both vertical and transverse directions. The damping ratio of spacer is set at 20%, based on [10]. The drag coefficient, C_D , is taken to be 1.25 as proposed in [11]. The density and Young's modulus of ice are chosen so that they correspond to glaze ice, i.e. $\rho_{ice} = 900$ kg/m³ and $E_{ice} = 10$ GPa. The spacer is assumed to be made of aluminum, thus its density and Young's modulus are: $\rho_s = 2700$ kg/m³ and $E_s = 70$ GPa respectively. For simplification, the spacer is assumed to be cylindrical with a length of $l_s = 0.5$ m and an average cross-sectional area of $A_s = 0.0021$ m². The sag of the unloaded cable is chosen as 6 m, while the thickness of ice accumulation is varied between 10 mm and 60 mm in

consecutive simulations. The ice load is identical on the two subconductors before shedding, and full ice shedding is modeled from either subconductor.

B. Comparison with a Former Model

Simulation results are compared with those obtained by a previously developed finite element model [6] by means of jump height of the unloaded cable at mid-span where the spacer is attached. The model of twin bundle in horizontal plane with one spacer constructed in [6] was applied to compute jump heights. Fig. 4 compares the results obtained by the two models. The increase of jump height with ice thickness is slightly slower according to the present model. This model predicts higher jumps at mid-span for lower ice loads; however, smaller jumps are obtained by applying this model following the shedding of higher ice loads.

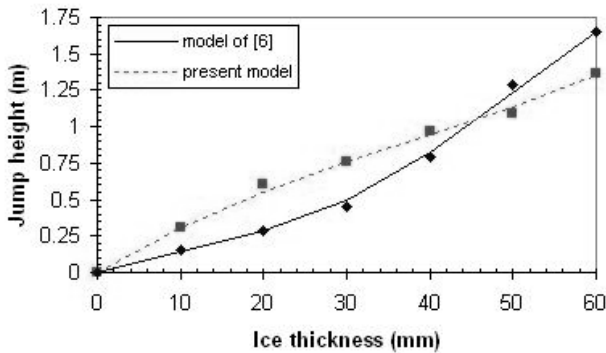


Fig. 4. Jump height of unloaded cable at spacer attachment point as computed by the present and a previously developed model

C. Rotation of Bundle and Forces Acting on Spacer

In order to simulate ice shedding from one subconductor, the cables are assumed to be in the loaded position initially, but the mass, stiffness and damping properties of the cable which ice sheds from are set as if that cable was bare. Simulations were carried out for a specific spacer characteristic, with rotation of spacer of $\varphi_{cr} = 16^\circ$ at the critical deformation where the arms are blocked.

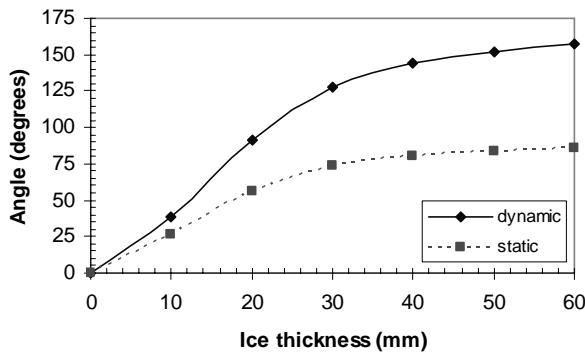


Fig. 5. Rotation angle of spacer during vibration and in static equilibrium

Fig. 5 shows the maximum rotation of the spacer during the vibration induced by the shedding of ice with different thicknesses. This figure also presents the angle of rotation in

the static equilibrium when either cable is bare and the other one is still covered by ice. The angle 90° means that the mid-point of the unloaded cable is pulled above that of the loaded one, with the spacer turned into vertical position. This angle is a limit for bundle rotation in static equilibrium when the difference between the loads on the two cables increases. However, under windy conditions the bundle rotation angle may exceed 90° as reported e.g. in [12]. Also, the peak value of this angle is significantly greater than 90° during the first cycle of the vibration after the shedding of ice with thickness greater than 20 mm, as shown in Fig. 5. However, the peaks in subsequent cycles decrease quickly due to cable damping. Time histories obtained after the shedding of a 40-mm-thick ice load are shown in Fig. 6. This figure shows clearly how the peaks in rotation angle decrease with time. The vibration of mid-points of the two cables in the vertical direction may also be observed. The sag of the unloaded cable, which is 6 m, increases up to 7.24 m when the cable is loaded with 40-mm-thick ice. As the vibration decays and the system approaches its equilibrium, the spacer becomes close to vertical position (80.4° in equilibrium); thus, the vertical projection of the distance between the two cables will also be close to 0.5 m, which is the spacer length. The time history of the force acting on the spacer is also shown in Fig. 6. A high peak appears in the first cycle, then peaks decrease fast in the next cycles. The spacer damping attenuates this peak force together with the high-frequency vibration which is superposed on the time-history curve.

Fig. 7 shows the peak forces acting on the spacer during the vibration due to the shedding of ice of different

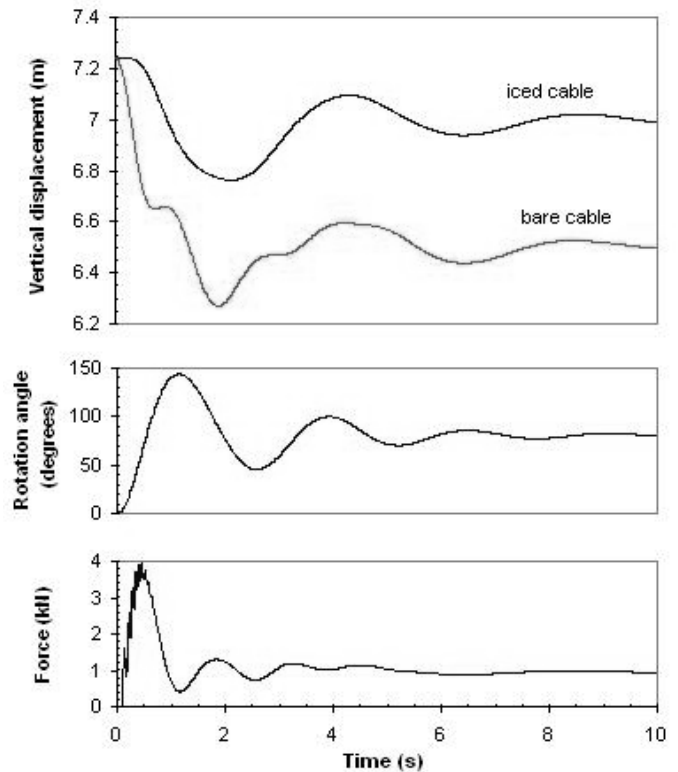


Fig. 6. Time history of vertical displacements of cables, rotation angle of spacer, and force in spacer following the shedding of 40-mm-thick ice load

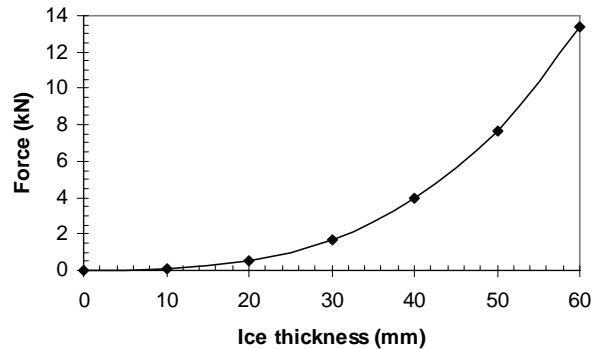


Fig. 7. The maximum force acting on the spacer during vibration

thicknesses. A comparison of Figs. 5 and 7 show that the rate of increase in the angle of rotation diminishes in the higher range of ice load, because further deformation of the system becomes more and more difficult, which results in steeper and steeper increase in the force developing in the spacer.

V. CONCLUSIONS

This paper presented a 4-DOF model of twin bundles of conductors including a spacer at mid-span. The model simulates vibration in the vertical plane of the spacer due to ice shedding. As compared to a previously developed finite element model, this model does not provide information about the dynamics of the cable at any location except at the spacer attachment point. However, if the question is limited to the behavior of the cable system in the vicinity of the spacers, then this model is easier to apply and computationally less costly.

From this study, recommendations for future work are: (i) development of more accurate spacer models by applying elastic and damping properties of specific spacers, (ii) extending the model to triple and quad bundles, and (iii) comparison of simulation results to experimental or field observations.

VI. ACKNOWLEDGMENT

This work was carried out within the framework of the NSERC/Hydro-Quebec/UQAC Industrial Chair on Atmospheric Icing of Power Network Equipment (CIGELE) and the Canada Research Chair on Engineering of Power Network Atmospheric Icing (INGIVRE) at Université du Québec à Chicoutimi. The authors would like to thank the CIGELE partners (Hydro-Québec, Hydro One, Électricité de France, Alcan Cable, K-Line Insulators, CQRDA and FUQAC) whose financial support made this research possible.

VII. REFERENCES

- [1] V. T. Morgan, D. A. Swift, "Jump height of overhead-line conductors after the sudden release of ice loads," *Proceedings of IEE*, vol. 111, no. 10, pp. 1736-1746, 1964.
- [2] A. Jamaledine, G. McClure, J. Rousselet, R. Beauchemin, "Simulation of Ice Shedding on Electrical Transmission Lines Using ADINA," *Computers & Structures*, vol. 47, no. 4/5, pp. 523-536, 1993.

- [3] M. Roshan Fekr, G. McClure, "Numerical modelling of the dynamic response of ice shedding on electrical transmission lines," *Atmospheric Research*, vol. 46, pp. 1-11, 1998.
- [4] ADINA R & D, *ADINA – Theory and Modeling Guide*, Watertown, MA, USA, 2003, Report ARD 03-7.
- [5] L. E. Kollar, M. Farzaneh, "Dynamic Analysis of Overhead Cable Vibrations as a Result of Ice Shedding," in *Proc. of 6th International Symposium on Cable Dynamics*, Charleston, SC, USA, 2005, pp. 427-434.
- [6] L. E. Kollar, M. Farzaneh, "Vibration of Bundled Conductors Following Ice Shedding," *IEEE Transactions on Power Delivery*, submitted in 2006.
- [7] P. Hagedorn, N. Mitra, T. Hadulla, "Vortex-Excited Vibrations in Bundled Conductors: A Mathematical Model," *Journal of Fluids and Structures*, vol. 16, no. 7, pp. 843-854, 2002.
- [8] CIGRE SCB2 WG11, "State of the Art Survey on Spacers and Spacer Dampers", *Electra* No. 277, August 2005.
- [9] H. M. Irvine, *Cable Structures*, MIT Press, Cambridge, MA, USA, 1981.
- [10] C. Hardy, P. Bourdon, "The Influence of Spacer Dynamic Properties in the Control of Bundle Conductor Motion," *IEEE Transactions on Power Apparatus and Systems*, vol. PAS-99(2), pp. 790-799, 1980.
- [11] A. B. Peabody, G. McClure, "Modeling the overhead power line post spring-damper using ADINA," in *Proc. of the 3rd MIT Conference on Computational Fluid and Solid Mechanics*, Cambridge, MA, USA, 2005.
- [12] A. T. Edwards, J. M. Boyd, "Bundle-Conductor-Spacer Design Requirements and Development of "Spacer-Vibration-Damper",," *IEEE Transactions on Power Apparatus and Systems*, vol. PAS-84(10), pp. 924-932, 1965.